

Energy Level Alignment in CdS Quantum Dot Sensitized Solar Cells Using Molecular Dipoles

Menny Shalom, Sven Rühle, Idan Hod, Shay Yahav, and Arie Zaban*

Institute of Nanotechnology & Advanced Materials, Department of Chemistry, Bar Ilan University, 52900 Ramat Gan, Israel

Received April 16, 2009; E-mail: zabana@mail.biu.ac.il

Nanocomposite solar cells are a promising low cost alternative to silicon *p-n* junction solar cells. Prominent examples are dye-sensitized solar cells (DSSCs) with record light to electric power conversion efficiencies above 10% and polymer based cells, which can reach efficiencies of ~5%.¹ In DSSCs dye molecules absorb photons and inject electrons from their excited state into the conduction band of a mesoporous TiO₂ film where they diffuse to a transparent conducting front contact while the oxidized dye is recharged by a redox electrolyte, which transports the positive charge to a Pt back electrode. Replacing the organic dye by inorganic quantum dots (QDs) has attracted a lot of attention due to the larger absorption coefficient of QDs and the tunability of the absorption spectrum by quantum size confinement.^{2–6} Sensitizing mesoporous TiO₂ electrodes with QDs can be done either in situ, where the absorber is directly grown onto the TiO₂ nanoparticles,⁷ or ex situ, where QDs are introduced into the mesoporous film and attached to the nanoparticle surface by linker molecules.^{8,9} A prerequisite to using QDs as absorbers in photovoltaic devices is their capability to inject charge carriers from their excited state into the adjacent electron and hole conducting media, (i.e., electrons into the TiO₂ and holes into the electrolyte) emphasizing the importance of energy level alignment. Molecular modification is a powerful tool to change the energy levels of bulk semiconductor surfaces;¹⁰ it has been used to improve the *I-V* characteristics of solar cells¹¹ as well as charge separation in QD polymer blends.¹² In DSSCs it was shown that the TiO₂ conduction band (CB) can be shifted with respect to the redox potential in a systematic fashion by cografing molecules with different dipole moments onto the TiO₂ surface.^{13,14} However systematic manipulation of the absorber energy levels in QD sensitized solar cells using molecular dipole moments has not been reported before. This alignment method opens the possibility to shift the energy levels of QDs, which normally do not inject, above the CB edge of the electron conducting medium.

Here we present a systematic shift of the energy levels of in situ grown CdS QDs with respect to the TiO₂ bands using molecules with different dipole moments. We have investigated CdS sensitized mesoporous and flat TiO₂ electrodes immersed in an aqueous polysulfide redox electrolyte. We shift the photoresponse onset using a series of benzenethiol (BT) derivatives which adsorb strongly to the CdS surface. It is shown that the solar cell photocurrent strongly depends on the molecular dipole moment, while the optical absorption spectrum of the sensitized electrodes remains unchanged.

Photovoltage spectroscopy (PVS) is a sensitive tool to detect the onset of electron injection from an absorber into the electron conductor such as TiO₂. PVS of flat TiO₂ electrodes sensitized with CdS QDs modified with BT derivatives is shown in Figure 1a.

The signal onset, which we define as the energy at which the PVS signal has reached 20% of its maximum value, shows a linear correlation with the molecular dipole moment. Table 1 summarizes

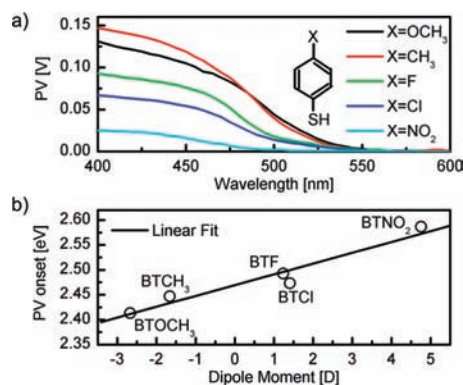


Figure 1. (a) Photovoltage spectroscopy (PVS) of flat TiO₂ electrodes sensitized with CdS quantum dots modified with BT derivatives, showing a dipole dependent PV signal. (b) PV onset plotted as a function of the molecular dipole moment. The least-squares fit (solid line) shows a linear dependence of the onset with the molecular dipole moment.

the dipole moments calculated for the free molecules. From Figure 1b we derive that the energy levels of in situ grown CdS QDs can be shifted by 21.7 meV/Debye with respect to the TiO₂ bands.

Incident photon to current efficiency (IPCE) measurements of flat electrodes are presented in Figure 2a, showing a similar trend like the PVS results. The signal onset becomes visible at shorter wavelengths due to the lower sensitivity of the IPCE at low injection rates. Due to the polydisperse size distribution of the in situ prepared QDs we do not observe a sharp signal onset as reported for monodisperse linker bound QD systems.⁸ The short circuit current density (*J*_{sc}) of both, the flat and the mesoporous (mp) CdS QD sensitized electrodes, recorded at an illumination intensity of 1 sun (100 mW/cm²) under simulated sunlight (AM 1.5G) are presented in Figure 2b. Schematic drawings of the flat and mesoporous solar cells are shown in the inset. All photocurrent measurements, IPCE and *J*_{sc}, show larger currents when the molecular dipole moment is pointing toward the QD. Only the BTNO₂ (dipole moment of 4.76 D) does not fit the dipole related trend, which can be attributed to the good surface wetting of the BTNO₂ modified QD with electrolyte. This is supported by contact angle measurements, showing a small angle for BTNO₂ modified QDs (Table 1), which

Table 1. Calculated Dipole Moments of the Investigated Benzenethiol Derivatives and Measured Contact Angles of Molecular Modified Flat CdS Sensitized TiO₂ Electrodes

molecule	name	dipole moment [D]	contact angle
4-methoxy BT	BTOCH ₃	-2.67	15°
4-methyl BT	BTCH ₃	-1.66	65°
4-fluoro BT	BTF	1.23	70°
4-chloro BT	BTCI	1.41	73°
4-nitro BT	BTNO ₂	4.76	20°

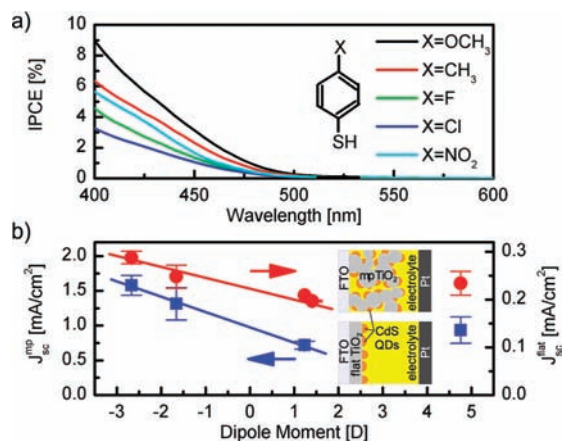


Figure 2. (a) Incident photon to current efficiency (IPCE) measurements of CdS QD sensitized flat TiO₂ electrodes, modified with a series of BT derivatives, show a dipole dependent photoresponse. (b) Dipole dependent short circuit current density of flat (●) and mesoporous CdS QD sensitized TiO₂ electrodes (■) measured at AM 1.5G illumination.

is improving the recharging of the QDs after electron injection into the TiO₂. The observed shift in the PVS onset provides strong evidence that the energy levels of the CdS QDs are shifted with

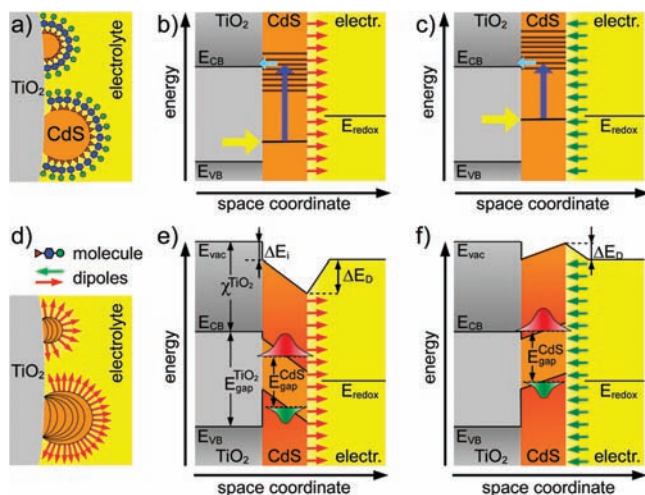


Figure 3. (a) Schematic drawing of sensitized TiO₂ with QDs of different size having a molecular modified surface. (b) Energy band diagram showing the ground and excited states of polydisperse CdS QDs. Molecular dipoles pointing away from the CdS surface shift the QD energy levels down, such that higher photon energies are required (dark blue arrow) to excite electrons into energy states which permit electron injection into the TiO₂ CB (light blue arrow). (c) Negative dipoles shift the QD levels up such that larger QDs, excited at lower photon energies, can also inject electrons into the TiO₂. (d) Schematic drawing of dipole modified QD surfaces, showing equipotential lines inside the dots. (e) Energy band diagram of an individual QD, showing the electron affinity χ and the valence and conduction band edge of TiO₂ (E_{CB} and E_{VB}). The local vacuum level E_{vac} includes an interface dipole ΔE_i at the TiO₂/CdS junction and the potential drop across the dipole layer ΔE_D . The electric field in the QD induced by the molecular dipole layer shifts the electron (red) and hole wave function (green) of the excited state toward lower energies such that electron injection into the TiO₂ is energetically hindered. (f) Negative dipoles shift the energy levels up such that electron injection into the TiO₂ CB becomes possible.

respect to the TiO₂ bands. The molecular modified CdS QD sensitized TiO₂ surface is schematically depicted in Figure 3a. An energy band diagram of polydisperse QDs, modified with positive molecular dipole moments (Figure 3b), shows a downward shift of the QD energy levels. Thus electron injection from excited states of larger QDs (with lower excited state energy levels) into the TiO₂ is energetically hindered, which leads to the observed shift in the PVS onset and to a lower current density at white light illumination. Negative dipoles shift the QD energy levels upward, enabling electron injection into the TiO₂ CB at lower excitation energies (Figure 3c), thus leading to larger photocurrents and a PVS onset at longer wavelengths.

In contrast to linker bound QDs we have grown the QDs directly onto the TiO₂ surface such that the TiO₂/QD interface remains unaffected upon molecular modification. The electrostatic potential within a QD is defined by its surrounding, schematically shown by equipotential lines in Figure 3d (see also Supporting Information). Energy band diagrams of one individual QD (Figure 3e and f) show the electrostatic field within the dot, caused by the molecular dipole layer. The energy levels of the (excited state) electron and hole wave functions shift as a function of the electrostatic field such that electron injection from the first excited state is either impossible (Figure 3e) or allowed (Figure 3f), depending on the molecular dipole.

We have demonstrated a systematic shift of QD energy levels with respect to an adjacent semiconductor using molecular dipoles, which is an important alignment tool for QD sensitized solar cells and QD based electronic devices in general.

Acknowledgment. S.R. acknowledges financial support from the European Unions FP 7 framework program. The authors thank Dr. Dan T. Major and Dr. Michal Weitmann for the calculation of the dipole moments.

Supporting Information Available: Experimental methods and absorption spectra are available free of charge via the Internet at <http://pubs.acs.org>.

References

- (1) Green, M. A.; Emery, K.; Hishikawa, Y.; Warta, W. *Prog. Photovoltaics* **2009**, *17*, 85–94.
- (2) Hodes, G. *J. Phys. Chem. C* **2008**, *112*, 17778–17787.
- (3) Kamat, P. V. *J. Phys. Chem. C* **2008**, *112*, 18737–18753.
- (4) Shalom, M.; Dor, S.; Rühle, S.; Grinis, L.; Zaban, A. *J. Phys. Chem. C* **2009**, *113*, 3895–3898.
- (5) de Mello Donega, C.; Hickey, S. G.; Wuister, S. F.; Vanmaekelbergh, D.; Meijerink, A. *J. Phys. Chem. B* **2003**, *107*, 489–496.
- (6) Niitsoo, O.; Sarkar, S. K.; Pejoux, C.; Rühle, S.; Cahen, D.; Hodes, G. *J. Photochem. Photobiol., A* **2006**, *181*, 306–313.
- (7) Gorer, S.; Hodes, G. *J. Phys. Chem.* **1994**, *98*, 5338–5346.
- (8) Kongkanand, A.; Tvrđy, K.; Takechi, K.; Kuno, M.; Kamat, P. V. *J. Am. Chem. Soc.* **2008**, *130*, 4007–4015.
- (9) Mora-Sero, I.; Gimenez, S.; Moehl, T.; Fabregat-Santiago, F.; Lana-Villareal, T.; Gomez, R.; Bisquert, J. *Nanotechnology* **2008**, *19*, 424007.
- (10) Cahen, D.; Kahn, A. *Adv. Mater.* **2003**, *15*, 271–277.
- (11) Gal, D.; Sone, E.; Cohen, R.; Hodes, G.; Libman, J.; Shanzer, A.; Schock, H. W.; Cahen, D. *Proc. Indian Acad. Sci., Chem. Sci.* **1997**, *109*, 487–496.
- (12) Soreni-Harari, M.; Yaacobi-Gross, N.; Steiner, D.; Aharoni, A.; Banin, U.; Millo, O.; Tessler, N. *Nano Lett.* **2008**, *8*, 678–684.
- (13) Rühle, S.; Greenshtein, M.; Chen, S. G.; Merson, A.; Pizem, H.; Sukenik, C. S.; Cahen, D.; Zaban, A. *J. Phys. Chem. B* **2005**, *109*, 18907–18913.
- (14) Neale, N. R.; Kopidakis, N.; van de Lagemaat, J.; Grätzel, M.; Frank, A. J. *J. Phys. Chem. B* **2005**, *109*, 23183–23189.

JA902770K